Advanced Powder Technology 34 (2023) 104075

Contents lists available at ScienceDirect

Advanced Powder Technology

journal homepage: www.elsevier.com/locate/apt

Original Research Paper

High-yield spray drying assembly and reactive properties of nanoenergetic mesoparticle composites

Mahbub Chowdhury [1], Pankaj Ghildiyal [1], Alex Rojas, Yujie Wang, Haiyang Wang, Michael R. Zachariah *

University of California, Riverside, CA 92521, United States

ARTICLE INFO

Article history:
Received 7 November 2022
Received in revised form 3 March 2023
Accepted 24 April 2023
Available online 12 May 2023

Keywords:
Spray drying
Energetic materials
Nanothermites
Particle assembly
Scalable production

ABSTRACT

Electrospray has been demonstrated to assemble fuel and oxidizer nanoparticles with a gas-generating binder into microscale particle composites. This approach results in reactivity enhancement of nanothermite systems by alleviating reactive sintering of the nanoparticle components due to rapid gasification. However, this method is not readily scalable and amenable to large-scale manufacturing due to its slow solution processing rates and the risks associated with the presence of high electric fields in the presence of electrostatic discharge-sensitive reactive materials. Here, we explore spray drying as an alternative approach to assemble Al/CuO nanoparticles into nitrocellulose (NC)-based mesoparticle composites and evaluate their energetic performance against physically mixed powders and electrosprayed mesoparticles. The spray dried mesoparticles show ~2–7-fold higher pressurization rates and shorter burn times than their physically mixed counterparts and follow a similar trend with electrospray. The higher reactivity of the mesoparticles is attributed to rapid gas generation and reduced sintering from the decomposition of the NC binder. We further demonstrate that spray drying generates mesoparticles with size (~1.5–4 μm), morphology, and reactivity enhancement similar to that from the electrospray method, while achieving remarkably high production rates (as high as ~275 g h^{-1}). Thus, this work presents spray drying as a highly scalable strategy to achieve reactivity enhancement and processability, thereby enabling high-yield manufacturing of energetic materials, which is a prelude to what might evolve into 3-D printing approaches for propellants.

1. Introduction

Nanoenergetic systems comprising of fuel and oxidizer components in the form of nanoscale particulates promise high energy density and reaction rates due to shorter diffusion length scales and high surface areas [1–6]. However, nanoparticle-based reactive systems present multiple challenges for practical, large-scale solid propellant applications. First, the high surface area of the nanoparticles dramatically increases the viscosity of the polymer-based formulations, which limits the maximum mass loadings that can be incorporated in propellant formulations [7,8]. Secondly, the nanoparticle components themselves undergo a loss of nanostructure due to reactive sintering prior to combustion, resulting in incomplete energy extraction and stunted reactivity [9,10]. These challenges become especially critical with rising demands for large-scale fabrication and additive manufacturing of nanoparticle-based solid propellants [11,12].

Assembling nanoscale components by encapsulating them in a gas-generating polymer binder into micron-size mesoparticle composites has been demonstrated as an effective strategy to overcome the aforementioned challenges [13,14]. These composites have been shown to exhibit high reactivity and shorter burn times due to enhanced fuel-oxidizer interfacial contact and reduced sintering due to early gas release [14–17]. The rapid gas generation has been proposed to de-aggregate the nanoparticles before combustion, thereby alleviating sintering and energy loss. In addition, due to their overall microscale structure, these composites can overcome processability issues inherent to nanoparticles while retaining and exploiting the benefits of their nanoscale components [13,16]. In other words, these composites combine the advantages of both the nano-as well as the micro-scale.

Despite these advantages, fabrication of mesoparticles composites has mostly been limited to small-scale electrospray-based techniques [11–16]. In a typical electrospray setup, the precursor solution is fed through a fine metallic capillary (nozzle) maintained

* Corresponding author.
E-mail address: mrz@engr.ucr.edu (M.R. Zachariah).
[1] Mahbub Chowdhury and Pankaj Ghildiyal have equal contribution.

https://doi.org/10.1016/j.apt.2023.104075

at high voltage, where the solution is nebulized into fine, charged droplets and driven through a high electric field to a grounded substrate. Subsequent solvent evaporation and coulombic droplet fissions cause the fuel and oxidizer particles to pack into monodisperse composite particles, typically ~ 2–10 μm. Previous studies have reported significantly low production rates (~1–100 mg h^{-1}) for electrospray generation of nanoparticles and composites [18,19]. This stems from the fact that an essential prerequisite for continuous electrospray of mesoparticles is the formation of a stable Taylor cone, that suffers from low solution processing rates (~100's of μL min^{-1}) and thus limits process scalability. Even though the use of multiple, parallel nozzles has been proposed as a strategy for scale-up, the technique is not amenable and straightforward for practical applications [20]. Moreover, the extremely high electric fields (a few kV cm^{-1}) employed in electrospray approaches raise additional safety concerns for the large-scale production of energetic materials.

Spray drying, on the other hand, circumvents the need for such high electric fields or low-throughput nozzles and, thus, presents a scalable and commercially viable alternative to electrospray. This technique has been established to be exceptionally adaptable and easy-to-replicate on a commercial scale [21]. In this approach, the precursor solution is nebulized into aerosol droplets that are subsequently dried into solid particles using a hot drying gas, as shown in Fig. 1.1 [22–24]. Laboratory-scale spray dryers have been shown to produce particle sizes in the range of 2–20 μm with production rates up to ~ 2–200 g h^{-1}[21,25–27]. Larger, industrial-scale dryers have the capability to scale-up the particle production process to exceptionally large rates (up to 2 tons a day) [26]. Notably, the resulting particle size range for spray drying (~2–25 μm) is ideal for generation of energetic mesoparticles, and since the particle sizes are similar to those generated by electrospray, a direct comparison and evaluation of their energetic performance can be made. Moreover, recent studies have shown that in addition to the formation of solid spherical composites, spray drying approaches can also be employed to generate alternative morphologies, such as hollow structures and superstructures[27–29].

In this paper, we demonstrate the formation of spray dried Al/CuO mesoparticle composites using nitrocellulose (NC) as the gas generating binder. The spray dried composites show higher reactivity than physical mixtures of the individual components, suggesting an enhancement effect due to local gas-generation in the composite particles. More importantly, we evaluated the production rate and particle size of the spray drying process under different conditions to assess its scalability for mesoparticle production. We observed that the production rate to be high as ~ 275 g h^{-1} (assembling materials with ~ 1100 kJ of stored energy per hour), showcasing its high throughput and comparison between spray dried and electrospray mesoparticles shows essentially no performance difference. These results present a promising and robust solution towards large-scale fabrication of nanostructured materials.

2. Material and methods

2.1. Materials

Al (ALEX, <50 nm, 67% active Al content) and CuO nanoparticles (~40 nm) were obtained from Argonide Corporation and US Research Nanomaterials, respectively. Collodion solution (4–8% in ethanol/diethyl ether) was obtained from Millipore Sigma and was dried to obtain solid nitrocellulose for further processing. N, N-dimethylformamide (DMF), 2-propanol (IPA), anhydrous diethyl ether (99.9%) and acetone were purchased from Fischer Scientific. Ethyl Alcohol (100% absolute undenatured) was purchased from Koptec.

2.2. Electrospray precursor preparation procedure

Desired amount of solid nitrocellulose binder was dissolved in ethanol and diethyl ether (volume ratio 1:1). To this solution, Al and CuO NPs were added stoichiometrically. The prepared sample was sonicated for 1 h and then magnetically stirred for 24 h. In a typical experiment for 100 mg ml^{-1} loading, 1.5 to 10 mg NC was dissolved in 0.5 mL ethanol and 0.5 mL diethyl ether followed by the addition of a stoichiometric amount of Al and CuO nanoparticles.

2.3. Electrospray

The reactant nanoparticles were assembled into microparticles with the electrospray process. The precursor solution was loaded into a 10 mL syringe (inner diameter 20.86 mm) with a stainless-steel needle (inner diameter: 0.43 mm). This syringe was placed in a syringe pump with a constant flow of 4.5 mL h^{-1}, and the distance between the needle and substrate was maintained at 10 cm. 10 kV (+) and 9 kV (-) were applied to the nozzle and substrate respectively, and the resultant droplets were evaporated while in flight from the nozzle to the substrate and deposited as solid particles. A schematic diagram of the electrospray setup is given in Fig. 2.1.

2.4. Formulation and spray drying of Al/CuO-NC mesoparticle composites

To prepare the formulations for spray drying, the desired amount of the NC binder was dissolved in a 3:5:2 DMF:IPA:acetone solvent mixture. Al and CuO NPs were then added to the solution according to the stoichiometry of the reaction (fuel/oxidizer equivalence ratio, ϕ, =1). The suspension was then sonicated for ~ 1 h, followed by a minimum of 24 h of stirring. The slurry was then shear mixed and sonicated during the process of spray drying to enable homogeneous particle mixing throughout the suspension. For spray drying the formulations, a Büchi B-290 Mini Spray Dryer was used in conjunction with a B-295 inert loop. Argon preheated at ~ 110 °C was used as the drying gas throughout the spray drying system. The prepared suspension was fed through a peristaltic pump at a 45% feeding rate (~12.5 mL min^{-1}) with an aspirator rate of 85% (~33 m^3 h^{-1}) and ~ 7 L min^{-1} of inlet gas flow. The particles were collected in a cyclone-based collector, which was electrostatically neutralized before sample collection. For the safe handling of materials, a low solid loading (10 mg mL^{-1}) was used while formulating the Al-CuO precursor solutions.

2.5. Conventional physical mixing

To prepare the physical mixtures, the NC solution (20 mg mL^{-1}, 0.7:1 DMF:acetone solvent mixture) was first spray dried at a drying temperature of 110 °C to obtain the NC powder. The NC powder was then mixed with Al and CuO NPs in hexane (10 mg L^{-1}), followed by sonication for ~ 1 h and drying overnight to obtain physically mixed Al/CuO-NC powders.

2.6. Combustion cell characterization

Al/CuO/NC samples were tested in a constant volume combustion cell (~20 cm^3). The experiments were conducted in the air and the initial pressure in the combustion cell was maintained at atmospheric pressure. The samples were ignited with a nichrome wire inside the chamber such that the wire only touches the center of the top surface of the powdered sample. The nichrome wire resistively heats to ignite the sample, and the sample is then allowed to self-propagate. An oscilloscope records the pressure

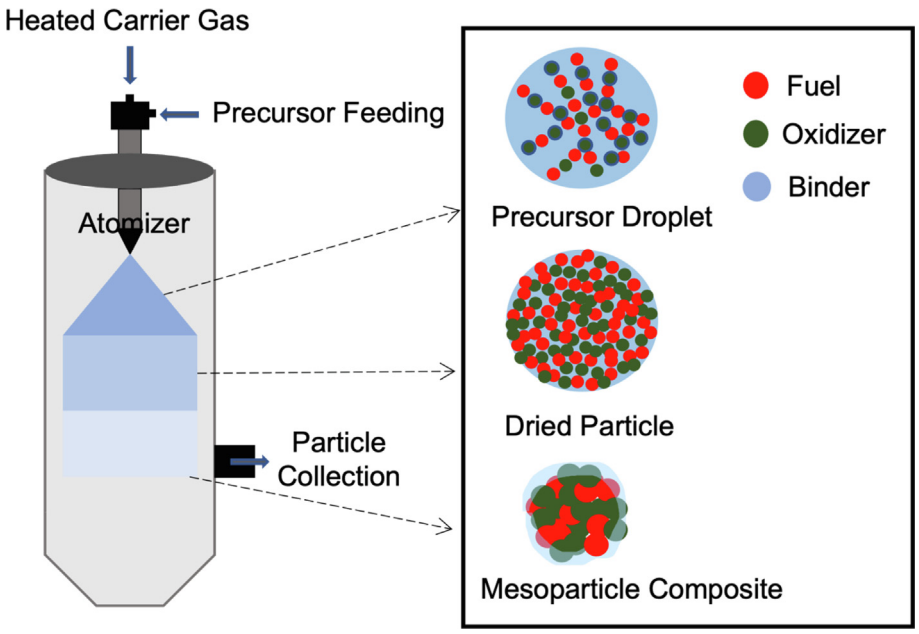

Fig. 1.1. Spray drying assembly of energetic mesoparticle composites.

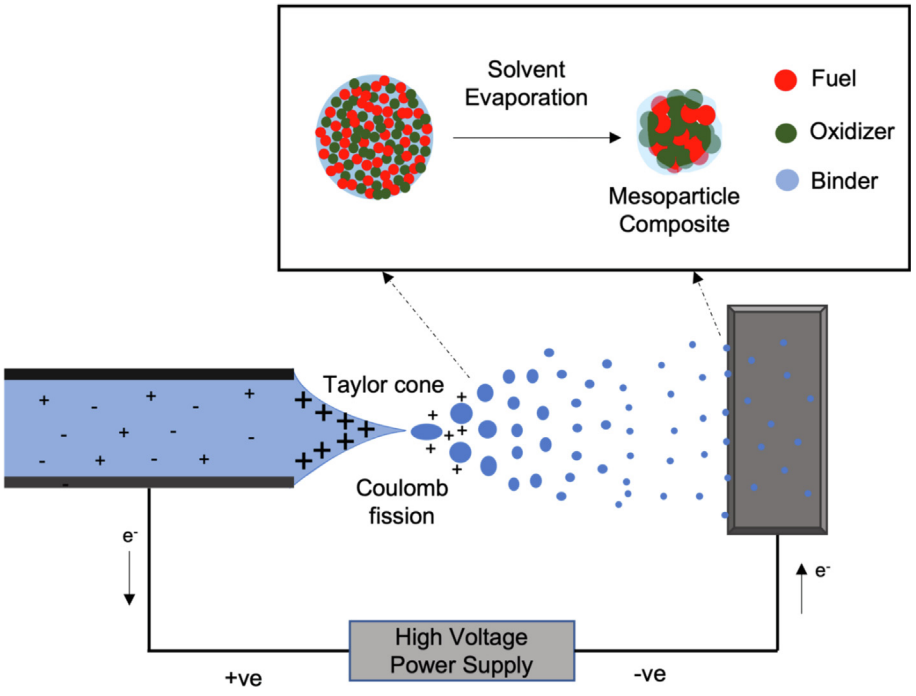

Fig. 2.1. Electrospray formation of nanostructured mesoparticles [30].

and optical signal and a high frequency pressure tranducer (PCB Piezoelectronics) was used to obtain the time dependent pressure signal. The optical emission from the reaction was focused by a convex lens and transferred to a photomultiplier tube (Hamamatsu) through a fiber optic cable. Peak pressure was divided by pressure rise time to get the pressurization rate. Burn time was defined at full width at half maximum of the optical emission. A minimum of three runs were carried out for each sample to obtain the average pressurization and burn characteristics.

2.7. Characterization

A Thermo-Fisher scientific, FEI NNS450 scanning electron microscope (SEM), operating at 18KV was used to characterize the morphology and the size of the microparticles. SEM energy-dispersive spectroscopy was used to evaluate the elemental homogeneity of the microparticles. SEM images using ImageJ software (v. 1.53) were used to extract particle size distributions with a nominal sample size of 50 mesoparticles.

3. Results and discussion

3.1. Spray drying and electrospray formation of Al/CuO/NC mesoparticle composites

In the spray drying process polymer encapsulated mesoparticles containing fuel and oxidizer nanoparticles aggregate during solvent evaporation in-flight and produce composite micron size particles.

Figs. 3.1 and 3.2 show the scanning electron microscopy (SEM) image for spray dried and electrosprayed Al-CuO/NC mesoparticles with varying NC content respectively, and Fig. 3.3 shows the size distribution of the mesoparticles obtained. The precursor solution containing 1.5 wt% NC produced very low number of spray dried discernible spherical mesoparticles but for electrospray, significant well formed mesoparticles can be seen with this concentration of NC. The average diameter of the particle was 1.5 μm, whereas the average particle diameter for electrosprayed mesoparticle was 3 μm for 1.5 wt%. NC content. Increasing the NC content from 1.5 wt% to 10 wt% increased the average mesoparticle size both for spray drying and electrospray. NC acts as a binder which can hold the aggregates of nanoparticle into a micron size structure that can retain the physical shape preventing breakdown. From Fig. 3.1, increasing the NC content to 2.75 wt% for spray drying extensively

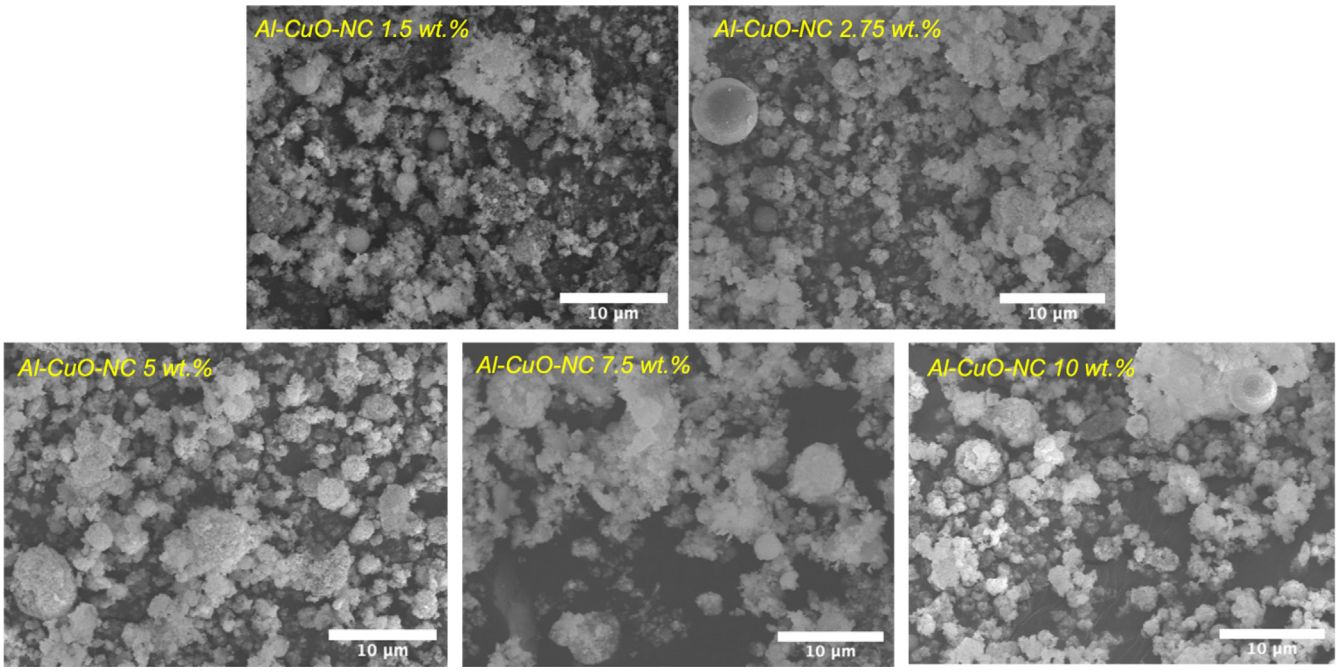

Fig. 3.1. SEM images of Spray dried Al/CuO-NC mesoparticles with different NC binder content (scale bars: 10 μm).

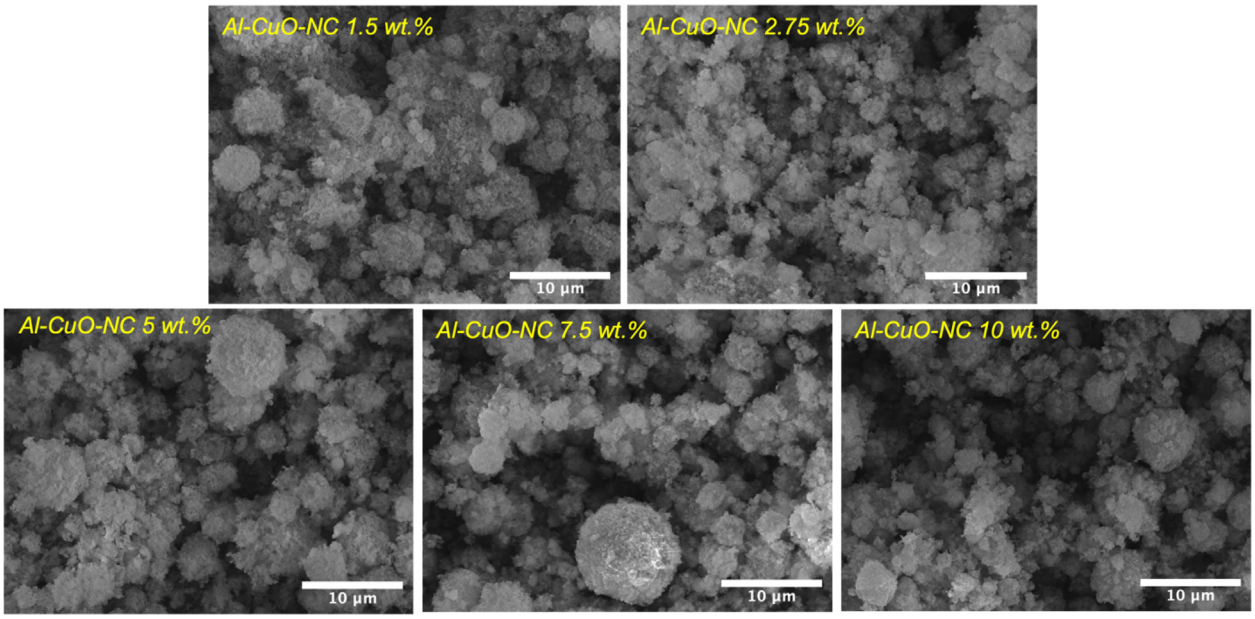

Fig. 3.2. SEM images of Electrosprayed Al/CuO-NC mesoparticles with different NC binder content (scale bars: 10 μm).

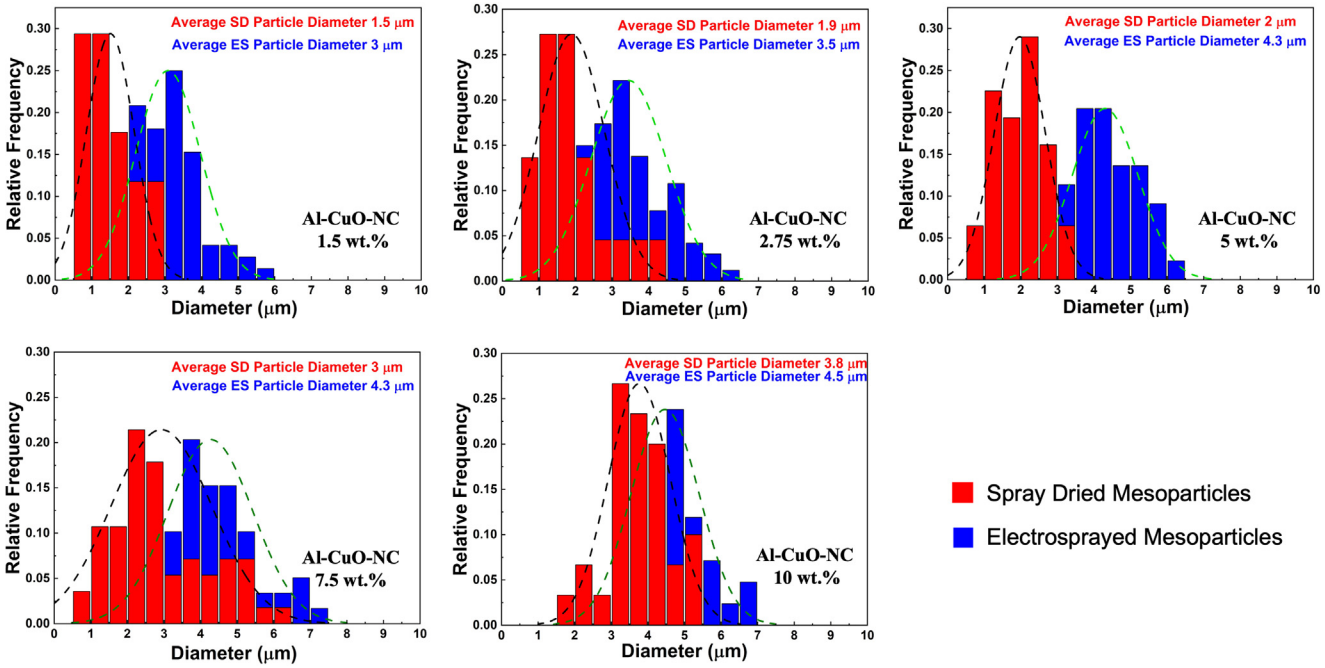

Fig. 3.3. Comparison of particle size distribution of Spray dried and Electrosprayed mesoparticles with different NC binder content.

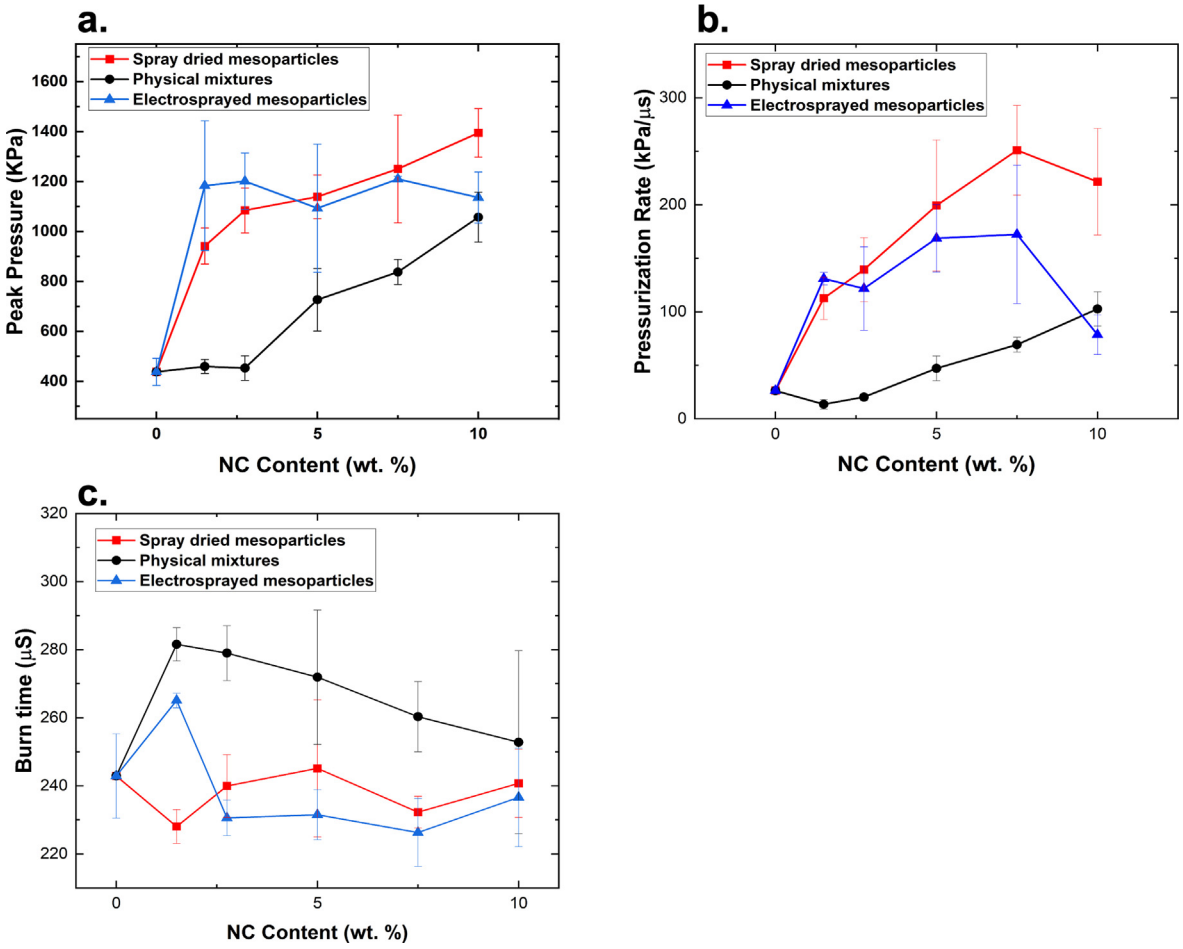

Fig. 3.4. Comparison of **(a)** peak pressure, **(b)** pressurization rate, and **(c)** burn time of spray dried Al/CuO-NC mesoparticle composites with electrosprayed mesoparticles and physical mixtures at different NC binder concentrations.

increased the number of formed spherical mesoparticles. Fig. 3.3 shows that increasing the NC content to 10 wt%, the average particle diameter increased to ~ 3.8 μm and ~ 4.5 μm for spray drying and electrospray respectively.

The size of the particles obtained from spray drying is comparable to the particles obtained from electrospray (3 ~ 4.5 μm). Elemental mapping (Figure S1.1) of the individual particles was obtained from X-ray energy dispersive spectrum (EDS), which

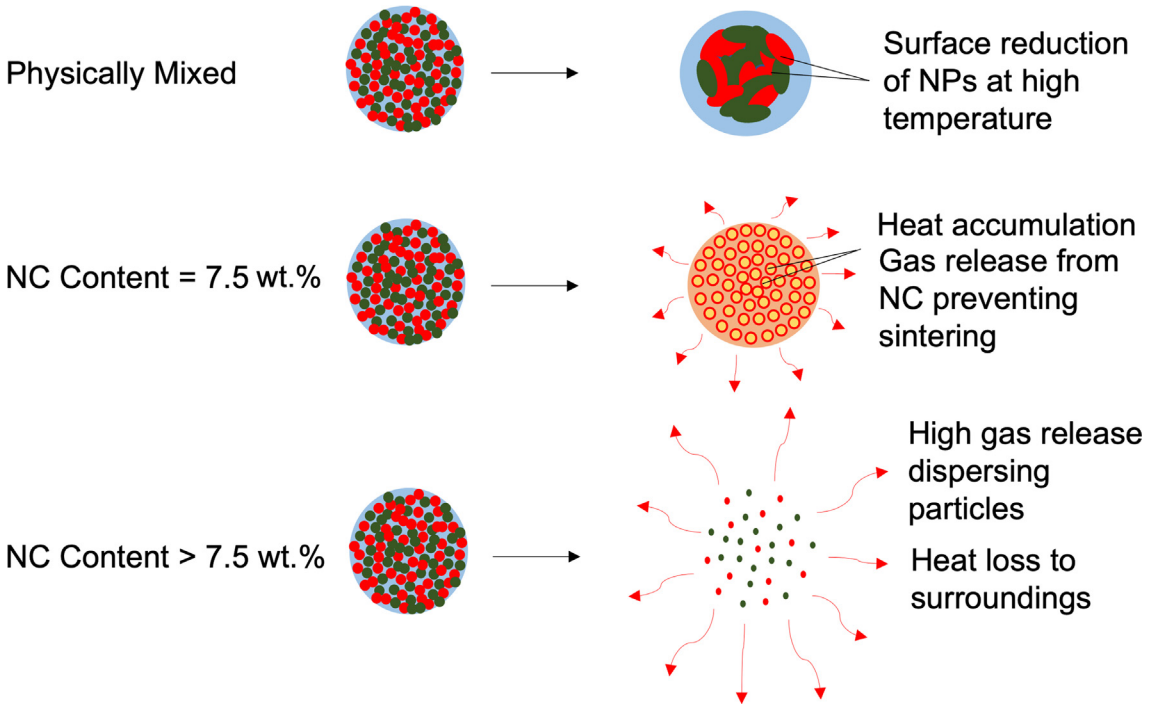

Fig. 3.5. Comparison among possible mechanisms for the combustion of physically mixed and mesoparticle thermites.

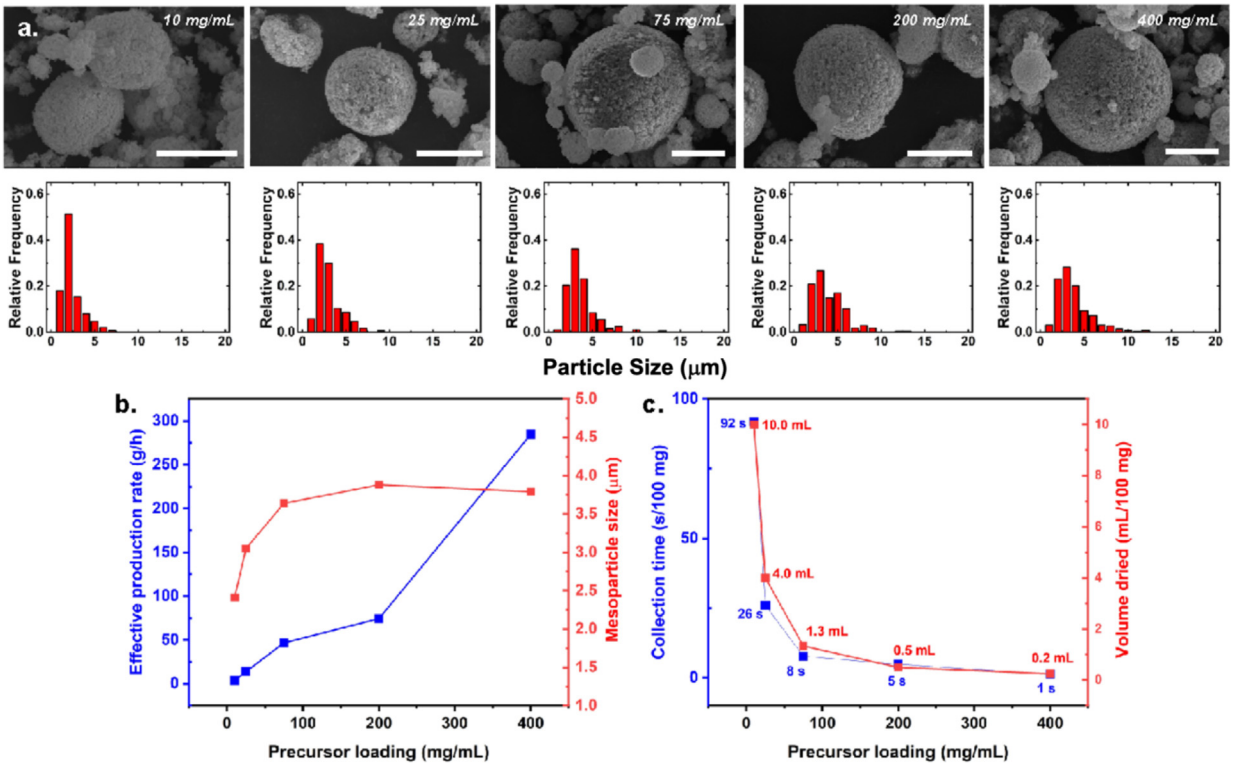

Fig. 3.6. (a) SEM images and the corresponding particle size distributions of CuO-NC mesoparticles fabricated under different precursor loading conditions (scale bars: 5 μm), (b) effect of precursor loading on the effective production rate and average mesoparticle size, and (c) total collection time and dried volume for mesoparticle formation for different solid loadings.

shows that Al and CuO are homogeneously mixed state similar to that obtained from the electrospray process. (Figure S1.2).

3.2. Combustion characteristics of spray dried Al/CuO-NC mesoparticles

Fig. 3.4 compares the peak pressure, pressurization rate and burn time between the mesoparticles from electrospray and spray drying approach along with their physically mixed counterparts as a function of the NC content obtained from the constant-volume combustion cell. The peak pressure is the highest pressure developed during the combustion and the pressurization rate is evaluated from the slope of a linear fit from the pressure rise point to the peak pressure. The combustion performance from spray dried and the electrosprayed Al-CuO/NC mesoparticles clearly outperforms their physically mixed counterparts. The peak pressure for spray dried mesoparticles showed ~ 1.3–2.4-fold enhancement and reached ~ 1400 KPa for 10 wt% of NC. The pressurization rate for spray dried mesoparticles exhibited ~ 2–7 times higher than physical mixtures, and it increased up to a NC content of 7.5 wt% (~250 KPa/μs). The spray dried mesoparticles also showed ~ 9–18% reduction in burn times. The combustion performance of the spray dried mesoparticles as can be seen in Fig. 3.4, closely track the behavior of electrosprayed mesoparticles, and thus spray drying offers all the advantages of electrospray but with a much more practical fabrication approach.

It can be seen from the Fig. 3.4 (b) and (c) that pressurization rate increases and burn time decreases up to 7.5 wt% NC both for spray dried and electrosprayed mesoparticles. This better combustion performance may suggest that fuel and oxidizer have better interfacial contact than their physically mixed state. Fig. 3.5 showing that physically mixed nanoparticles undergo sintering at high temperatures. This agglomeration of the nanoparticles causes the reduction in the interfacial surface area of the metal and oxidizer, thus retarding the reactivity.

NC is an energetic source with low decomposition temperature (170 °C) that produces gas at low temperature and prevents sintering. Due to less heat loss, the heat of reaction is trapped inside the mesoparticle structure (Fig. 3.5) and accumulates heat, which causes the reaction to be self-propagating. This likely explains the higher reactivity of the mesoparticle composites up to 7.5 wt % NC. Increasing the NC content further decreases the pressurization rate and increases the burn time because the NC has a lower energy content causing overall energy degradation. Furthermore, too much gas generation causes the structure of the mesoparticle to break down and makes the reactants further apart such that it loses heat to the surroundings, as shown in Fig. 3.5. The pressurization rate at 10 wt% NC content decreases to ~220 KPa/μs for spray drying which is ~250 KPa/μs for 7.5 wt% NC and the corresponding burn time increases from ~230 μs to ~240 μs.

3.3. Production rate, particle size, and different mesoparticle systems obtained

The scalability of the spray drying process was evaluated by studying the effect of total solid loading in the precursor solutions on mesoparticle size and production rate. Since these measurements were expected to produce large material quantities, for safety reasons, the composites were prepared with only CuO and NC as the components without the fuel (Al NPs). Fig. 3.6a shows that the particles obtained under different precursor loading conditions show a consistent spheroidal morphology with particle size ranging from ~2.5 to ~ 3.8 μm. The average particle size increases only slightly (~2.5 to ~3.8 μm) and remains constant at 200 mg/mL loadings and higher. The marginal increase in particle size despite a 40-fold increase in mass loading of the precursor suggests that the particle size is likely limited by the initial droplet size as generated from the shearing of the liquid by the high-pressure spray gas [31]. Due to rapid and efficient evaporation of the droplet by the hot drying gas, the particles are locked. The effective production rate was estimated from the amount of material collected and the time taken for deposition in the collection vessel. As expected, Fig. 3.6b shows an increasing trend of production rate with increasing solid loading in the precursor solutions. The highest production rate achieved in this study is ~275 g h^{-1}, demonstrating the extremely high scalability for the production of reactive mesoparticle composites while maintaining a consistent size and morphology. For comparison, as discussed earlier, the solution processing and drying rates in a typical electrospray deposition setup are considerably lower (~1 mL h^{-1}) since the solution nebulization and droplet formation necessitate the formation of a stable Taylor cone. In contrast, a typical spray drying setup can process and dry extremely large solvent volumes (~900 mL h^{-1}), making it considerably more scalable, while achieving similar reactivity enhancement and particle structure as electrospray assembly. Moreover, the absence of high electric fields in a spray dryer should make large scale manufacturing of reactive mesoparticles significantly safer than the electrospray approach.

4. Conclusions

This current study presents the spray drying technique as a highly scalable and straightforward technique to fabricate micron size particles composed of nanocomponents. Mesoparticles from spray drying exhibited similar size and spherical morphology to the electrosprayed mesoparticles. Spray dried mesoparticles also have the similar reactivity enhancement as the electrosprayed particles. These mesoparticles show enhanced reactivity over the physically mixed counterparts because of rapid gas generation, reduced particle sintering and better interfacial contact. The spray drying technique can achieve very high production rates (~275 g h^{-1}) and an effective drying rate of ~720 mL hr^{-1}, which is ~160 fold enhancement over electrospray approach without compromising reactivity and unchanged size distribution and morphology. The spray drying method can achieve the same result as electrospray but in a more scalable manner. Due to this high processability spray dried mesoparticle can be used as building blocks for nanocomposite films.

CRediT authorship contribution statement

Mahbub Chowdhury: Conceptualization, Investigation, Methodology, Writing – original draft, Visualization, Formal analysis. **Pankaj Ghildiyal:** Conceptualization, Investigation, Methodology, Writing – original draft, Visualization, Formal analysis. **Alex Rojas:** Investigation. **Yujie Wang:** Investigation. **Haiyang Wang:** Methodology, Investigation, Conceptualization. **Michael R. Zachariah:** Supervision, Conceptualization, Methodology.

Declaration of Competing Interest

The authors declare that they have no known competing financial interests or personal relationships that could have appeared to influence the work reported in this paper.

Acknowledgments

This work was supported by a grant from the ONR. The authors also want to acknowledge valuable discussions with Dr. Aaron Mason from NAWS-China Lake. We also want to thank CFAMM

at the University of California, Riverside for supporting microscopy instrumentation.

Appendix A. Supplementary data

Supplementary data to this article can be found online at https://doi.org/10.1016/j.apt.2023.104075.

References

[1] M. Mursalat, C. Huang, B. Julien, M. Schoenitz, A. Esteve, C. Rossi, E.L. Dreizin, Low-Temperature Exothermic Reactions in Al/CuO Nanothermites Producing Copper Nanodots and Accelerating Combustion, ACS Appl. Nano Mater. 4 (2021) 3811–3820, https://doi.org/10.1021/acsanm.1c00236.

[2] H. Wang, P. Biswas, M.R. Zachariah, Direct Imaging and Simulation of the Interface Reaction of Metal/Metal Oxide Nanoparticle Laminates, J. Phys. Chem. C. 126 (2022) 8684–8691, https://doi.org/10.1021/acs.jpcc.2c00156.

[3] Y. Chen, W. Ren, Z. Zheng, G. Wu, B. Hu, J. Chen, J. Wang, C. Yu, K. Ma, X. Zhou, W. Zhang, Reactivity adjustment from the contact extent between CuO and Al phases in nanothermites, Chem. Eng. J. 402 (2020), https://doi.org/10.1016/j.cej.2020.126288.

[4] P. Ghildiyal, P. Biswas, S. Herrera, F. Xu, Z. Alibay, Y. Wang, H. Wang, R. Abbaschian, M.R. Zachariah, Vaporization-Controlled Energy Release Mechanisms Underlying the Exceptional Reactivity of Magnesium Nanoparticles, ACS Appl. Mater. Interfaces. 14 (2022) 17164–17174, https://doi.org/10.1021/acsami.1c22685.

[5] B. Julien, J. Cure, L. Salvagnac, C. Josse, A. Esteve, C. Rossi, Integration of Gold Nanoparticles to Modulate the Ignitability of Nanothermite Films, ACS Appl. Nano Mater. 3 (2020) 2562–2572, https://doi.org/10.1021/acsanm.9b02619.

[6] P. Ghildiyal, F. Xu, A. Rojas, Y. Wang, M. Chowdhury, P. Biswas, S. Herrera, R. Abbaschian, M.R. Zachariah, Magnesium-Enhanced Reactivity of Boron Particles: Role of Mg/B $_{2\ O}$ 3 Exothermic Surface Reactions, Energy Fuels. 37 (2023) 3272–3279, https://doi.org/10.1021/acs.energyfuels.2c02347.

[7] T. Hanemann, D.V. Szabó, Polymer-Nanoparticle Composites: From Synthesis to Modern Applications, Materials. 3 (2010) 3468–3517, https://doi.org/10.3390/ma3063468.

[8] Z. Xu, R.K. Singh, J. Bao, C. Wang, Direct Effect of Solvent Viscosity on the Physical Mass Transfer for Wavy Film Flow in a Packed Column, Ind. Eng. Chem. Res. 58 (2019) 17524–17539, https://doi.org/10.1021/acs.iecr.9b01226.

[9] R.J. Jacob, D.L. Ortiz-Montalvo, K.R. Overdeep, T.P. Weihs, M.R. Zachariah, Incomplete reactions in nanothermite composites, J. Appl. Phys. 121 (5) (2017) 054307, https://doi.org/10.1063/1.4974963.

[10] H. Wang, D.J. Kline, M.R. Zachariah, In-operando high-speed microscopy and thermometry of reaction propagation and sintering in a nanocomposite, Nat. Commun. 10 (2019) 3032, https://doi.org/10.1038/s41467-019-10843-4.

[11] C. Ru, F. Wang, J. Xu, J. Dai, Y. Shen, Y. Ye, P. Zhu, R. Shen, Superior performance of a MEMS-based solid propellant microthruster (SPM) array with nanothermites, Microsyst. Technol. 23 (2017) 3161–3174, https://doi.org/10.1007/s00542-016-3159-x.

[12] H. Wang, J. Shen, D.J. Kline, N. Eckman, N.R. Agrawal, T. Wu, P. Wang, M.R. Zachariah, Direct Writing of a 90 wt% Particle Loading Nanothermite, Adv. Mater. 31 (2019) 1806575, https://doi.org/10.1002/adma.201806575.

[13] G. Young, H. Wang, M.R. Zachariah, Application of Nano-Aluminum/Nitrocellulose Mesoparticles in Composite Solid Rocket Propellants, Propellants Explos. Pyrotech. 40 (2015) 413–418, https://doi.org/10.1002/prep.201500020.

[14] H. Wang, G. Jian, W. Zhou, J.B. DeLisio, V.T. Lee, M.R. Zachariah, Metal Iodate-Based Energetic Composites and Their Combustion and Biocidal Performance, ACS Appl. Mater. Interfaces. 7 (2015) 17363–17370, https://doi.org/10.1021/acsami.5b04589.

[15] H. Wang, G. Jian, G.C. Egan, M.R. Zachariah, Assembly and reactive properties of Al/CuO based nanothermite microparticles, Combust. Flame. 161 (2014) 2203–2208, https://doi.org/10.1016/j.combustflame.2014.02.003.

[16] R.J. Jacob, B. Wei, M.R. Zachariah, Quantifying the enhanced combustion characteristics of electrospray assembled aluminum mesoparticles, Combust. Flame. 167 (2016) 472–480, https://doi.org/10.1016/j.combustflame.2015.09.032.

[17] W. Zhao, X. Wang, H. Wang, T. Wu, D.J. Kline, M. Rehwoldt, H. Ren, M.R. Zachariah, Titanium enhanced ignition and combustion of Al/I2O5 mesoparticle composites, Combust. Flame. 212 (2020) 245–251, https://doi.org/10.1016/j.combustflame.2019.04.049.

[18] A. Gomez, D. Bingham, L. de Juan, K. Tang, Production of protein nanoparticles by electrospray drying, J. Aerosol Sci. 29 (1998) 561–574, https://doi.org/10.1016/S0021-8502(97)10031-3.

[19] A.J. Rulison, R.C. Flagan, Synthesis of Yttria Powders by Electrospray Pyrolysis, J. Am. Ceram. Soc. 77 (1994) 3244–3250, https://doi.org/10.1111/j.1151-2916.1994.tb04577.x.

[20] A.J. Rulison, R.C. Flagan, Scale-up of electrospray atomization using linear arrays of Taylor cones, Rev. Sci. Instrum. 64 (1993) 683–686, https://doi.org/10.1063/1.1144197.

[21] I.C. Kemp, T. Hartwig, P. Hamilton, R. Wadley, A. Bisten, Production of fine lactose particles from organic solvent in laboratory and commercial-scale spray dryers, Dry. Technol. 34 (2016) 830–842, https://doi.org/10.1080/07373937.2015.1084314.

[22] K.L.A. Cao, F. Iskandar, E. Tanabe, T. Ogi, Recent Advances in the Fabrication and Functionalization of Nanostructured Carbon Spheres for Energy Storage Applications, KONA Powder Part. J. (2022) 2023016, https://doi.org/10.14356/kona.2023016.

[23] H. Zhou, R. Pujales-Paradela, P. Groppe, S. Wintzheimer, K. Mandel, Tuning the Morphology of Spray-Dried Supraparticles: Effects of Building Block Size and Concentration, Part. Part. Syst. Charact. 39 (2022) 2200127, https://doi.org/10.1002/ppsc.202200127.

[24] T.T. Nguyen, M. Miyauchi, A.M. Rahmatika, K.L.A. Cao, E. Tanabe, T. Ogi, Enhanced Protein Adsorption Capacity of Macroporous Pectin Particles with High Specific Surface Area and an Interconnected Pore Network, ACS Appl. Mater. Interfaces. 14 (2022) 14435–14446, https://doi.org/10.1021/acsami.1c22307.

[25] G.D. Park, J. Lee, Y. Piao, Y.C. Kang, Mesoporous graphitic carbon-TiO2 composite microspheres produced by a pilot-scale spray-drying process as an efficient sulfur host material for Li-S batteries, Chem. Eng. J. 335 (2018) 600–611, https://doi.org/10.1016/j.cej.2017.11.021.

[26] R.C. Suryaprakash, F.P. Lohmann, M. Wagner, B. Abel, A. Varga, Spray drying as a novel and scalable fabrication method for nanostructured CsH_2PO_4, Pt-thin-film composite electrodes for solid acid fuel cells, RSC Adv. 4 (2014) 60429–60436, https://doi.org/10.1039/C4RA10259B.

[27] A. Carné-Sánchez, I. Imaz, M. Cano-Sarabia, D. Maspoch, A spray-drying strategy for synthesis of nanoscale metal–organic frameworks and their assembly into hollow superstructures, Nat. Chem. 5 (2013) 203–211, https://doi.org/10.1038/nchem.1569.

[28] K.L.A. Cao, Y. Kitamoto, F. Iskandar, T. Ogi, Sustainable porous hollow carbon spheres with high specific surface area derived from Kraft lignin, Adv. Powder Technol. 32 (2021) 2064–2073, https://doi.org/10.1016/j.apt.2021.04.012.

[29] H. Canziani, F. Bever, A. Sommereyns, M. Schmidt, N. Vogel, Roughly Spherical: Tailored PMMA–SiO_2 Composite Supraparticles with Optimized Powder Flowability for Additive Manufacturing, ACS Appl. Mater. Interfaces. 13 (2021) 25334–25345, https://doi.org/10.1021/acsami.1c02264.

[30] H. Wang, G. Jian, S. Yan, J.B. DeLisio, C. Huang, M.R. Zachariah, Electrospray Formation of Gelled Nano-Aluminum Microspheres with Superior Reactivity, ACS Appl. Mater. Interfaces. 5 (2013) 6797–6801, https://doi.org/10.1021/am401238t.

[31] I.C. Kemp, R. Wadley, T. Hartwig, U. Cocchini, Y. See-Toh, L. Gorringe, K. Fordham, F. Ricard, Experimental Study of Spray Drying and Atomization with a Two-Fluid Nozzle to Produce Inhalable Particles, Dry. Technol. 31 (2013) 930–941, https://doi.org/10.1080/07373937.2012.710693.